

Raman Spectroscopic Investigation of H₂, HD, and D₂ Physisorption on Ropes of Single-Walled, Carbon Nanotubes

Keith A. Williams,* Bhabendra K. Pradhan, Peter C. Eklund,[†] Milen K. Kostov, and Milton W. Cole

Physics Department, The Pennsylvania State University, 104 Davey Laboratory, University Park, Pennsylvania 16802

(Received 23 April 2001; published 4 April 2002)

We have observed the *S*- and *Q*-branch Raman spectra of H₂, HD, and D₂ adsorbed at 85 K and pressures up to 8 atm on single-walled, carbon nanotubes (SWNT). Comparative data for H₂ on graphite and C₆₀ were also collected. Frequency-downshifted and upshifted features were observed in the *Q*-branch spectra of H₂ on C₆₀ and SWNT. These shifts are small and are therefore inconsistent with charge transfer. An H₂-surface potential with van der Waals and electrostatic terms was developed and used to estimate the shifts in the frequency of the *Q*(0) transition of H₂ adsorbed in two types of sites. These calculations corroborate the experimental findings and indicate physisorption in multiple sites of the SWNT ropes.

DOI: 10.1103/PhysRevLett.88.165502

PACS numbers: 61.46.+w, 68.43.-h

Single-walled, carbon nanotubes (SWNT) are nanoporous, all-surface macromolecules which are being widely investigated as storage media for H₂ [1,2]. Desorption experiments suggest the presence of a high-energy binding site for H₂ in purified and sonicated SWNT material, which has been proposed to indicate charge transfer [3]. On the other hand, transport data for SWNT suggest that H₂ physisorbs [4]. To probe the interaction on the molecular level, we have collected *S*- and *Q*-branch Raman spectra of H₂, HD, and D₂ adsorbed on SWNT at 85 K and pressures up to 8 atm. The magnitude of the shifts in the *Q*-branch frequencies of the adsorbed species is a measure of the strength of the adsorption potential; for physisorption, the shifts should be small, while in the event of charge transfer, the shifts should be ~ 2000 cm⁻¹ per electron [5].

Using a two-step, oxidative, and acid reflux technique, we obtained SWNT samples containing minimal amorphous and multishell carbon (<15 wt %) and residual metal catalyst (<10 wt %, <2 at. %), as determined by temperature programmed oxidation (IGA-3, Hiden Inc.). This material was annealed in a vacuum of better than 10⁻⁷ Torr at 1200 K for 24 h; such high-temperature “de-gassing” was recently shown to remove the carboxylic and related functional groups occluding the SWNT ends and side walls [6]. The resulting material was pressed against In foil and inserted in an optical pressure cell, which was placed in a cryostat (Janis Corp. Model VPF 700, 77-700 K) with a gas line to the cell. The cell was valved to a diffusion pump and to the cylinders of H₂ (ultrahigh purity, 99.999%, MG Industries), HD (97.4 mole%, with 1.4% H₂ and 1.2% D₂, Isotec Inc.), and D₂ (ultrahigh purity, 99.999%, MG Industries). In separate experiments, samples of C₆₀ powder (Alfa Aesar, 99.9%, packed under Ar) and freshly cleaved, pyrolytic graphite (Alfa Aesar) were loaded into our cell.

Raman spectra were collected in the backscattering geometry, with $\lambda_{\text{air}} = 514.53$ nm excitation provided by a mixed-gas, Ar/Kr-ion laser (Coherent Inc., Innova Spectrum). The incident beam was focused through the win-

dows of the cryostat and pressure cell onto the sample surface. Backscattered Rayleigh light was rejected by a holographic “supernotch” filter (Kaiser, Inc.), and Raman light was focused through a 25 μm slit into a single-grating monochromator (Instruments S.A. HR460, grating: 1800 grooves/mm) equipped with a CCD. To calibrate our spectra and correct for instrumental nonlinearity, one Hg and several pairs of Ne emission lines close to the *Q*-branch lines of H₂, D₂, and HD were used. The Ar, Hg, and Ne frequencies were taken from Refs. [7] and [8].

For all data we report, the sample temperature was 85 ± 5 K, and the pressure of the adsorbate gas on the sample was increased from vacuum to as high as 8 atm, in the case of H₂ and D₂, and to 5 atm in the case of HD. Typical *S*- and *Q*-branch spectra are shown in Figs. 1 and 2; we use the notation *S*(*J*) and *Q*(*J*) to denote transitions, in which *J* is the initial state. The frequencies, ν_{ads} , of the observed *S*- and *Q*-branch transitions are given in Table I; these values were determined by fitting Voigt-profile functions to

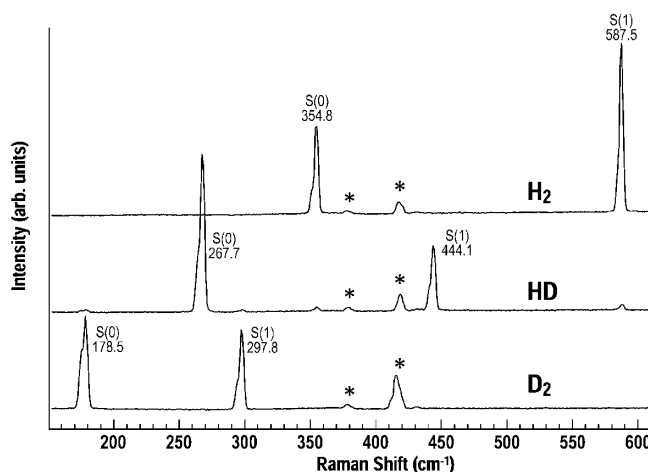


FIG. 1. *S*-branch data for H₂, HD, and D₂ on SWNT at 8, 5, and 8 atm, respectively. Asterisks indicate unrelated lines due to external calibration sources.

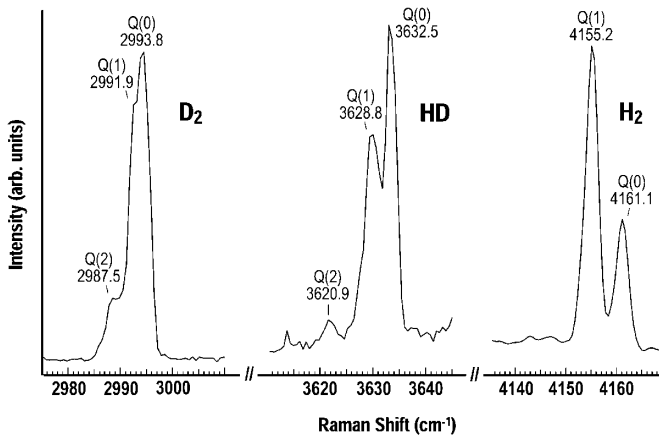


FIG. 2. Q -branch data for H_2 , HD, and D_2 on SWNT at 8, 5, and 8 atm, respectively. For comparisons of these peak positions with the frequencies of the free molecules, see Table I.

the spectra using Humlíček's algorithm [9]. Also provided in Table I are the frequencies, ν_{free} , of these transitions for free molecules, from Ref. [5].

Our S -branch data suggest freely rotating molecules in the gas phase, and are in good agreement with recent inelastic neutron scattering data [10]. Small, downshifted shoulders are evident in the S -branch lines, but our experimental resolution is insufficient to quantify these effects. The Q -branch data for HD and D_2 contain prominent bands which are slightly upshifted from the free-molecule frequencies (see Table I); due to the small splitting of the $J = 0$ and $J = 1$ bands, the peak substructure could not be resolved. Data for H_2 in SWNT are considerably more illu-

TABLE I. Frequencies ν_{ads} of the observed S - and Q -branch transitions of H_2 , HD, and D_2 adsorbed on SWNT at 8, 5, and 8 atm, respectively. Also indicated are the free-molecule frequencies (ν_{free}) from Ref. [5]; the difference is indicated by $\Delta\nu$.

Adsorbate species	Transition	ν_{free} (cm $^{-1}$)	ν_{ads} (cm $^{-1}$)	$\Delta\nu$ (cm $^{-1}$)
H_2	$Q(0)$	4160.5	4162.3	+1.8
			4161.1	+0.6
			4159.3	-1.2
	$Q(1)$	4154.4	4156.4	+2.0
			4155.2	+0.8
			4153.5	-0.9
			4153.5	-0.9
$S(0)$	354.4	354.8	+0.4	
		587.0	587.5	+0.5
HD	$Q(0)$	3629.8	3632.5	+2.7
			3628.8	+0.6
			3620.5	+0.4
	$S(0)$	267.1	267.7	+0.6
			443.1	444.1
D_2	$Q(0)$	2993.5	2993.8	+0.3
			2991.4	+0.5
			2987.2	+0.3
	$S(0)$	179.1	178.5	-0.6
			297.5	297.8

minating, and are shown in expanded form in Fig. 3 at two pressures, along with comparative data for C_{60} and highly oriented pyrolytic graphite (HOPG) collected at 85 ± 5 K and 4 atm. Best fits (solid lines) to the data in Fig. 3 were computed using a sum of Voigt components (dashed lines).

The surface area of HOPG is very small, so the signal strength from adsorbed molecules should be negligible. Therefore, we assign the bands observed at 4161.3 and 4155.4 cm $^{-1}$ to gas-phase H_2 near the surface; these frequencies are in reasonable agreement with the those reported in Ref. [11]. The gas-phase components should also be present in the data on C_{60} and SWNT, and so our analysis of these data proceeded by inserting components of frequency and width equal to those observed on HOPG, and then introducing separate Voigt components to describe the additional bands. Consistent with this approach, we noted an approximately twofold increase in the relative intensities of the bands attributed to gas-phase species, as the pressure was increased from 4 to 8 atm. In our analysis of the data on SWNT at 8 atm, the positions of the bands attributed to the gas phase were allowed to vary, and the frequencies were found to be ~ 0.1 cm $^{-1}$ lower, again consistent with Ref. [11]. In addition to the gas-phase components, the data for C_{60} and SWNT contain downshifted and upshifted bands absent in the HOPG data. We ascribe these components to adsorption in the interstices, internal pores, or corrugated outer surfaces of the respective lattices. Neutron powder diffraction work by Fitzgerald *et al.*, has indicated the existence of an adsorbed phase in the octahedral sites of fcc- C_{60} [12]; presumably, these sites are partially filled under the conditions of our study and account for the lower-frequency component present in our Q -branch data for H_2 on C_{60} . The number of fitting parameters was reduced by setting equal the linewidth parameters of equally spaced pairs of $Q(0)$ and $Q(1)$ peaks. All parameters were then refined until χ^2 was minimized and the frequencies were obtained. Our confidence in the

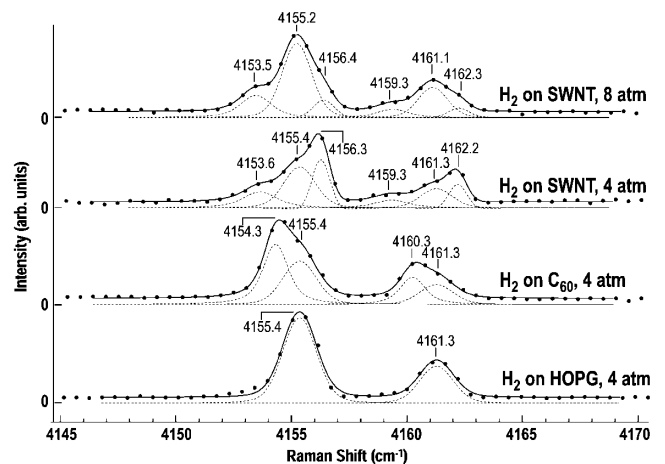


FIG. 3. Q -branch data for H_2 on SWNT at 8 and 4 atm, together with data for C_{60} and HOPG at 4 atm.

number of Voigt components introduced for each data set is affirmed by the relative intensities between “pairs” of Voigt components: $I_{Q(1)}/I_{Q(0)} = 2.2\text{--}2.5$, similar to the equilibrium orthopara ratio at 85 K. Also, the $Q(1)$ - $Q(0)$ spacing we find between these pairs ($5.8\text{--}6.0\text{ cm}^{-1}$) is consistent with the value ($\sim 5.97\text{ cm}^{-1}$) reported in Ref. [11].

Based on shifts observed in the tangential Raman bands of SWNT material previously dosed with H_2 , partial electron transfer from SWNT to the H_2 adsorbate has been proposed [3]. Our experiment is uniquely suited to looking for such effects, given the extreme sensitivity of the H_2 stretching frequency on the molecular charge state. Contrary to reports on certain zeolites and oxides [13], no strongly shifted Q -branch lines were observed on SWNT or C_{60} . This would seem to rule out charge transfer under our experimental conditions.

To predict the magnitudes of the stretching-mode shifts which arise from purely physical adsorption of H_2 , we have constructed an interaction potential and estimated the frequency shifts in two types of adsorption geometries in SWNT ropes. In one geometry, the surface is taken to be flat—representative of the outer and inner surfaces of individual SWNT. In the other, “confined” geometry, the H_2 is positioned between three surfaces, which is the situation in the interstitial channels of a SWNT rope. In both cases, the component surfaces were taken to be flat, an approximation which should not greatly affect the result.

Our potential is a sum of C-H van der Waals interactions, U_{LJ} , and the electrostatic interaction, U_{el} , of the H_2 static multipole moments with the static screening charges induced on the graphene surface [14]. Because the low-frequency dielectric response of graphene is metallic [15], the screening charges may be represented by full image charges displaced from the graphene sheet by a distance z_0 . Using a result for U_{el} which depends on the angular orientation (θ) of the molecule axis with respect to the surface normal, the electrostatic interaction may be expressed in terms of the H_2 quadrupole (Θ) and hexadecapole (Φ) moments [14]. The holding potential may then be written $V(z_c, \cos\theta) = U_{el} + U_{LJ}(z_1) + U_{LJ}(z_2)$, where the z_i are the perpendicular distances of the H atoms from the surface, and the $U_{LJ}(z_i)$ are the corresponding, pairwise, van der Waals interactions, which are assumed to be of Lennard-Jones (12-6) form. For simplicity, we smear out the C atoms along the surface. In this approximation,

$$U_{LJ}(z) = 2\pi\vartheta\epsilon_{\text{C-H}}\sigma_{\text{C-H}}^2 \left[\frac{2}{5} \left(\frac{\sigma_{\text{C-H}}}{z} \right)^{10} - \left(\frac{\sigma_{\text{C-H}}}{z} \right)^4 \right], \quad (1)$$

where $\vartheta = 0.38\text{ \AA}^{-2}$ is the surface density of the C atoms. We adopted the values $\epsilon_{\text{C-H}} = 2.26\text{ meV}$, $\sigma_{\text{C-H}} = 2.76\text{ \AA}$ [16]. The most uncertain parameter in our potential is z_0 [17]. To estimate this parameter, we computed the minimum of the C- H_2 potential at the equilibrium distance z_{eq} , where H_2 is preferentially oriented flat

against the surface. In the case of graphene, the isotropic C- H_2 holding potential has the same functional form as Eq. (1), with a minimum at $z_{\text{eq}} = \sigma_{\text{C-H}_2}$. Using $\epsilon_{\text{C-H}_2} = 42.8\text{ K}$ and $\sigma_{\text{C-H}_2} = 2.97\text{ \AA}$ [18], the resulting well depth is 46.6 meV and $z_0 = 1.36\text{ \AA}$, consistent with previous *ab initio* and empirical estimates for this system [19].

For the study of H_2 in the ICs, we adapted a potential developed for a single nanotube [20]. The dispersion part of this potential ignores many-body effects, considers the C atoms to be smeared on the surface, and is isotropic. The total potential for an IC was obtained by summing this potential over an assembly of three nanotubes and azimuthally averaging the result.

The electrostatic portion of the potential in the ICs contains two contributions, denoted U_1 and U_2 , which arise, respectively, from the interaction of the H_2 quadrupole moment with the local electrostatic field of the SWNT, and the interaction of the H_2 static multipole moments with the screening charges induced on the surface. U_1 is given by the usual relation for the electrostatic energy of a quadrupole in a nonuniform field, and was calculated from first principles for “zigzag” SWNT with radius $R = 6.9\text{ \AA}$ [21]. To evaluate U_2 , we included the H_2 quadrupole moment (the first nonzero permanent moment of an axial quadrupole), and the hexadecapole moment. The problem is quite complicated, so we introduce three simplifications. Because of the small size of H_2 , we consider its multipoles to be “pointlike.” Next, to simplify the geometry of the IC, we represent the SWNT walls with graphene planes. The locations of the image charges are determined by the boundary condition requiring that the potential be zero at each plane. Finally, we assumed that the graphene planes are perfectly conducting, so that the static and dynamic responses are represented by images. We adopted the same value for z_0 and the same form for the interaction as in the previous case. To compute the vibrational frequency shift, the total holding potential U must be expressed as a function of the relative bondlength change, $\xi = (r - r_e)/r_e$, relative to the equilibrium value, r_e , and also of the configuration τ of the molecule. Given a sufficiently small surface interaction, one can treat U and the anharmonic terms in the potential energy function of free H_2 as perturbations to the harmonic oscillator Hamiltonian [22]. Using first- and second-order perturbation theory, the change in the frequency of the fundamental ($n = 0 \rightarrow n = 1$) transition due to U is [22,23]:

$$\Delta\omega = \Delta\omega_{1\leftarrow 0} = \frac{B_e}{\hbar\omega_e} \langle U'' - 3aU' \rangle_\tau + O\left(\frac{B_e}{\hbar\omega_e}\right)^2. \quad (2)$$

in which B_e is the equilibrium rotational constant, a is the anharmonicity, primes denote derivatives with respect to ξ , and the angled brackets denote the average over all τ . The expressions for $\Theta(\mathbf{r})$ and $\Phi(\mathbf{r})$ were derived via a model in which the electron cloud is concentrated

between the nuclei rather than about each individual nucleus. Assuming an H_2 bondlength of 0.71 \AA , and placing the electrons symmetrically on the molecular axis, separated by 0.48 \AA , the experimental value of the H_2 quadrupole moment is reproduced. From this model, we find $\Theta \sim r^2$ and $\Phi \sim r^4$, for small changes in ξ about r_e . Regarding the orientational dependence, U' and U'' are functions of the z displacement of molecular center-of-mass, and of the polar (θ) and azimuthal (ϕ) angles. U depends on z_c , so the translational and rotational parts of $U'(z_c; \theta, \phi)$, $U''(z_c; \theta, \phi)$ do not decouple exactly. To separate the variables, we treat the interaction of translational and rotational modes in a mean-field manner [24]. The effective interaction was computed by averaging the derivatives of Eq. (2) over the center-of-mass vibrations of the molecule. Treating these as modes of a simple harmonic oscillator, the rms deviations in the z position are found to be $\delta z_{\text{rms}} = 0.298 \text{ \AA}$ on a single graphene surface, and $\delta z_{\text{rms}} = 0.15 \text{ \AA}$ for H_2 in an IC. Next, to compute $\langle U' \rangle_\tau$ and $\langle U'' \rangle_\tau$, variations were performed with respect to r in the adsorption potential for different τ . Finally, we averaged over all orientations (θ, ϕ) of the molecular axis.

Using the values $a = -1.6$ and $B_e/\hbar\omega_e = 0.0138$ [23], we find that for the case of H_2 adsorbed on graphene, our procedure predicts an upshift of $\Delta\omega_{1\leftarrow 0} = 1.4 \text{ cm}^{-1}$ ($\langle 3aU' \rangle = -126.2 \text{ cm}^{-1}$, $\langle U'' \rangle = -28.3 \text{ cm}^{-1}$). In contrast, for H_2 adsorbed in an IC, we predict a downshift of $\Delta\omega_{1\leftarrow 0} = -2.9 \text{ cm}^{-1}$ ($\langle 3aU' \rangle = 168.0 \text{ cm}^{-1}$, $\langle U'' \rangle = -42.2 \text{ cm}^{-1}$). We expect similar results for D_2 : the same potential parameters and quadrupole moment may be assumed, though a and $B_e/\hbar\omega_e$ are smaller and should produce smaller shifts. In the case of HD, the center of mass and charge do not coincide, leading to a larger Lennard-Jones contribution to the potential and a larger upshift.

In summary, we have observed several lines within the S - and Q -branch Raman spectra of H_2 , HD, and D_2 adsorbed on SWNT; the observed frequency shifts are small and consistent with physisorption. Both down- and upshifted features are evident in the Q branch, an effect we ascribe to H_2 adsorbed in two different types of sites in a SWNT rope. An interaction potential was developed to estimate the frequency shifts of the adsorbate stretching modes in two kinds of geometries similar to those found in SWNT ropes. In agreement with our experimental data, downshifted and upshifted modes are predicted, depending on the geometry of the adsorption site, and the shifts are small. Our calculations demonstrate that the experimental data are consistent with purely physical adsorption, without charge transfer.

We wish to thank Vin Crespi, Roger Herman, John Lewis, and Dragan Stojkovic for their generous contributions to this work. This work was funded by the Army Research Office and the Office of Naval Research.

*Present address: Technische Universiteit Delft, Department of Applied Physics, Lorentzweg 1, 2628 CJ Delft, The Netherlands.

†To whom correspondence should be addressed.

Email address: pce3@psu.edu

- [1] M. S. Dresselhaus, K. A. Williams, and P. C. Eklund, *MRS Bull.* **24**, 45–50 (1999).
- [2] A. C. Dillon and M. J. Heben, *Appl. Phys. A* **72**, 133–142 (2001).
- [3] M. J. Heben, A. C. Dillon, T. Gennett, J. L. Alleman, P. A. Parilla, K. M. Jones, and G. L. Hornyak, in *MRS Symposia Proceedings No. 633* (Materials Research Society, Pittsburgh, 2001), p. A9.1.1-11.
- [4] C. K. W. Adu, G. U. Sumanasekera, B. K. Pradhan, H. E. Romero, and P. C. Eklund, *Chem. Phys. Lett.* **337**, 31–35 (2001).
- [5] K. P. Huber and G. Herzberg, *Molecular Spectra and Molecular Structure: IV. Constants of Diatomic Molecules* (Van Nostrand Reinhold, New York, 1979).
- [6] A. Kuznetsova, D. B. Macwhinney, V. Naumenko, J. T. Yates, Jr., J. Liu, and R. E. Smalley, *Chem. Phys. Lett.* **321**, 292–296 (2000).
- [7] G. Norlén, *Phys. Scr.* **8**, 249–268 (1973).
- [8] K. Burns, K. B. Adams, and J. Longwell, *J. Opt. Soc. Am.* **40**, 339–344 (1950).
- [9] J. Humlíček, *J. Quant. Spectrosc. Radiat. Transfer* **27**, 437–444 (1982).
- [10] C. M. Brown, T. Yildirim, D. A. Neumann, M. J. Heben, T. Gennett, A. C. Dillon, J. L. Alleman, and J. E. Fischer, *Chem. Phys. Lett.* **329**, 311–316 (2000).
- [11] A. D. May, G. Varghese, J. C. Stryland, and H. L. Welsh, *Can. J. Phys.* **42**, 1058–1069 (1964).
- [12] S. A. Fitzgerald, T. Yildirim, L. J. Santodonato, D. A. Neumann, J. R. D. Copley, and J. J. Rush, *Phys. Rev. B* **60**, 6439–6451 (1999).
- [13] W. C. Conner, in *Physical Adsorption: Experiment, Theory, and Applications*, edited by F. Fraissard, NATO ASI, Ser. C, Vol. 491 (Kluwer Academic, Boston, 1997).
- [14] L. W. Bruch, *Surf. Sci.* **125**, 194 (1983).
- [15] H. R. Philipp, *Phys. Rev. B* **16**, 2896 (1977).
- [16] W. B. J. M. Janssen, T. H. M. van den Berg, and A. van der Avoird, *Phys. Rev. B* **43**, 5329 (1991).
- [17] F. Y. Hansen, L. W. Bruch, and S. E. Roosevelt, *Phys. Rev. B* **45**, 11 238 (1992).
- [18] S. C. Wang, L. Senbetu, and C. W. Woo, *J. Low Temp. Phys.* **41**, 611 (1980).
- [19] H. Y. Kim and M. W. Cole, *Phys. Rev. B* **35**, 3990 (1987).
- [20] G. Stan and M. W. Cole, *Surf. Sci.* **395**, 280 (1998).
- [21] These calculations were performed using the PARATEC package developed at U.C. Berkeley.
- [22] A. D. Buckingham, *Proc. R. Soc. A* **248**, 169 (1959).
- [23] R. M. Herman and S. Short, *J. Chem. Phys.* **48**, 1266 (1968).
- [24] A. D. Novaco and J. P. Wroblewski, *Phys. Rev. B* **39**, 11 364 (1989).
- [25] G. Herzberg, *Molecular Spectra and Molecular Structure: I. Spectra of Diatomic Molecules* (Van Nostrand Reinhold, New York, 1950).